UNIVERSIDAD DE CUENCA
FACULTAD DE INGENIERÍA
MAESTRÍA EN ECOHIDROLOGÍA

"How vegetation, soils, and precipitation control passive and dynamic storage change in high–elevation tropical catchments?"

AUTOR:

ING. PATRICIO XAVIER LAZO JARA

0104433966

DIRECTOR:

ING. PATRICIO JAVIER CRESPO SÁNCHEZ, PhD

0102572773

ASESORES:

ING. GIOVANNY MAURICIO MOSQUERA ROJAS, MSc.

0104450911

TRABAJO DE TITULACIÓN PREVIO A LA OBTENCIÓN DEL TÍTULO DE:
MAGÍSTER EN ECOHIDROLOGÍA

CUENCA – ECUADOR

2018

ABSTRACT

Understanding how tropical montane catchments store and release water is crucial for water resource management at surrounding elevations and downstream populations. Nevertheless, although research in montane tropical ecosystems has focused on streamflow generation, a lack of knowledge regarding catchments' water storage remains. Consequently, this study focuses on the investigation of catchment storage and the factors controlling its spatial variability in seven páramo catchments (0.20–7.53 km^2) located in south Ecuador. We used a hydrometeorological, water stable isotopic, and soils' hydrophysical properties dataset collected during Nov 2011–October 2014 to estimate catchments' passive (*PasS*) and dynamic (*DynS*) storages. We also investigated relations between these storages and landscape and hydrometric variables using linear regression analysis. The catchments' *PasS* and *DynS* were 313–617 mm and 29–35 mm, respectively. Catchments' *PasS* increased as their areal proportion of wetlands (Histosol soils) increased, and their *DynS* increased as the intensity of precipitation increased. Results also showed that *PasS* estimations using different methodologies were in agreement. Altogether, results evidence: 1) that only 6–10% of the catchments' mixing storage (*DynS*/*PasS*) is hydrologically active in their water balance, 2) the importance of wetlands for the provisioning of the catchments' *PasS*, and 3) the influence of the constant input of low intensity precipitation to sustain the wetlands recharge, and thus, the year–round water supply of páramo catchments. Findings that are crucial towards improvement of soil, vegetation, and water resources management in the páramo and other environments where the presence of peaty–like soils dominates.

Keywords: páramo soils, passive storage, dynamic storage, Neotropical alpine wetlands, peatlands, Andosols and Histosols

Abbreviations:

DynS – Dynamic storage

DynS$_{(ES)}$ – Event scale *DynS*

DynS$_{(LT)}$ – Long–term *DynS*

ET$_a$ – Actual evapotranspiration

ET$_{a(cum)}$ – Cumulative *ET*$_a$

ET$_o$ – Reference evapotranspiration

f – conversion factor from *ET*$_o$ to *ET*$_a$

MTT – Mean transit time

P – Precipitation

P$_{(cum)}$ – Cumulative *P*

PasS – Passive storage

PasS$_{(HP)}$ – *PasS* estimated from the soils' hydrophysical properties

PasS$_{(Q)}$ – *PasS* estimated from the streamflow MTT

PasS$_{(S)}$ – *PasS* estimated from the soils' MTT

Q – Discharge

Q$_{(cum)}$ – Cumulative *Q*

Q$_f$ – Normalized fractional *Q*

S(t) – Water balance based storage volume at time *t*

S$_f$ – Normalized fractional *storage*

TB – Tracer–based

TTD – Transit time distribution

WBB – Water balance based

ZREO – Zhurucay River Ecohydrological observatory

Patricio Xavier Lazo Jara

RESUMEN

Comprender como las cuencas de montaña tropicales almacenan y liberan agua es crucial para el manejo de recursos hídricos en las poblaciones aledañas. Sin embargo, a pesar de que la investigación en ecosistemas andinos se ha enfocado en la generación de escorrentía, todavía existe un vacío de conocimiento en el almacenamiento hídrico de las cuencas. Consecuentemente, este estudio se enfoca en la investigación del almacenamiento hídrico y los factores que controlan su variabilidad espacial en siete cuencas de páramo (0.2-7.53 km^2) ubicadas en el sur del Ecuador. Para esto se utilizaron datos hidrometeorológicos, de isótopos estables, y propiedades hidrofísicas de suelos recolectadas durante Noviembre 2011-Octubre 2014 para estimar el almacenamiento pasivo (*PasS*) y dinámico (*DynS*). También se analizó las relaciones entre estos almacenamientos y variables hidrométricas usando regresión lineal. El *PasS* y *DynS* de las cuencas fueron de 313-617 mm y 29-35 mm, respectivamente. El *PasS* incrementa al aumentar la proporción de Histosoles en la cuenca, y el *DynS* incrementa al aumentar la intensidad de la precipitación. Además, las estimaciones de *PasS* usando distintas metodologías concuerdan. Juntos estos resultados evidencian: 1) solo del 6-10% del almacenamiento mezclado de la cuenca (*DynS*/*PasS*) está hidrológicamente activo en el balance hídrico, 2) la importancia de los Histosoles al aprovisionar el *PasS*, y 3) la influencia del ingreso constante de precipitación de baja intensidad en mantener la recarga de los Histosoles, y así, el suministro de agua anual en las cuencas de páramo. Estos hallazgos son clave para mejorar el manejo de recursos hídricos.

Palabras clave: suelos de páramo, almacenamiento pasivo, almacenamiento dinámico, Andosoles, Histosoles.

Patricio Xavier Lazo Jara

Index

Patricio Xavier Lazo Jara

CLÁUSULA DE LICENCIA Y AUTORIZACIÓN PARA PUBLICACIÓN EN EL REPOSITORIO INSTITUCIONAL

Patricio Xavier Lazo Jara

CLÁUSULA DE PROPIEDAD INTELECTUAL

Patricio Xavier Lazo Jara, autor/a del trabajo de titulación "How vegetation, soils, and precipitation control passive and dynamic storage change in high–elevation tropical catchments?", certifico que todas las ideas, opiniones y contenidos expuestos en la presente investigación son de exclusiva responsabilidad de su autor.

Cuenca, 26 de febrero de 2018

Patricio Xavier Lazo Jara

C.I: 0104433966

Patricio Xavier Lazo Jara

ACKNOWLEDGMENTS

Patricio Xavier Lazo Jara

1. INTRODUCTION

Mountainous ecosystems provide key water–related services for downstream ecosystems and populations worldwide (Viviroli *et al.*, 2007; Asbjornsen *et al.*, 2017). This is particularly true for headwater tropical ecosystems, such as the Andean Páramo, which occupies over 30,000 km^2 of northern South America (Hofstede *et al.*, 2003; Wright *et al.*, 2017) and sustains the economy of millions of people in the region (IUCN, 2002). Among the variety of ecosystem services provided by the Páramo, its high water production and regulation capacity are two of the most important (Poulenard *et al.*, 2003; Buytaert, 2004). While recent Páramo hydrology research has focused on the investigation of the factors controlling the water production capacity of this ecosystem (e.g., Roa–García and Weiler, 2010; Buytaert and Beven, 2011; Crespo *et al.*, 2011, 2012, Mosquera *et al.*, 2015, 2016a, 2016b; Correa *et al.*, 2017; Polk *et al.*, 2017), the factors controlling its water regulation capacity have not been yet studied in detail.

Catchments' water regulation is highly influenced by their capacity to store and release water (Mcnamara *et al.*, 2011). As such, in the last decade, there has been an increasing interest within the hydrological science community towards improving our understanding of catchment water storage (hereafter referred to as 'catchment storage'). For instance, the study of catchment storage has helped improve our general understanding of the streamflow–storage relationships (e.g., Spence, 2007; Soulsby and Tetzlaff, 2008; Kirchner, 2009; Soulsby *et al.*, 2011; Tetzlaff *et al.*, 2014); how storage regulation and storage–discharge hysteresis depends on the antecedent wetness, flow rates, and catchment scale (Davies and Beven, 2015). These findings in turn, have been extremely useful as basis for the enhancement of the structure of hydrological models (e.g., Sayama and McDonnell, 2009; Nippgen *et al.*, 2015; Soulsby *et al.*, 2015; Birkel and Soulsby, 2016).

Notwithstanding, direct quantification of catchment storage remains difficult because of its largely unobservable nature (Hale *et al.*, 2016) and the marked internal (i.e., subsurface) spatial heterogeneity within and among catchments (Soulsby *et al.*, 2008; Seyfried *et al.*, 2009). In response to this, different approaches such as gravimetric techniques (Hasan *et al.*, 2008; Rosenberg *et al.*, 2012), cosmic ray soil moisture observations (Heidbüchel *et al.*, 2015), soil moisture measurements (Grant *et al.*, 2004; Seyfried *et al.*, 2009), streamflow recession analysis (Kirchner, 2009; Birkel *et al.*, 2011), water balance based (WBB), and tracer–based (TB) techniques (e.g., stable isotopes) (Birkel *et al.*, 2011; Mcnamara *et al.*, 2011; Hale *et al.*, 2016) have been applied in order to investigate these important feature of the hydrologic cycle. Among these, the combination of techniques has proven to provide the most valuable insights into water storage in catchments (Staudinger *et al.*, 2017). The combination of WBB and TB methods, for example, has allowed for an indirect quantification of dynamic storage (storage that is determined by the fluxes of water into and out of the catchment over a given period of time; Sayama *et al.*, 2011; hereafter referred as *DynS*) and passive storage (the subsurface volume of water stored within the catchment that mixes with incoming precipitation , Dunn *et al.*, 2010; Birkel *et al.*, 2011, hereafter refered as *PasS*). However, to date, only few studies have investigated storage combining different techniques (e.g., Pfister *et al.*, 2017; Staudinger *et al.*, 2017).

Apart from the quantification of catchment storage, the investigation of how catchment features (e.g., rainfall temporal variability, vegetation, soils, geology) affect its spatio–temporal variability remains an open but fundamental question in hydrological science (Mcnamara *et al.*, 2011). The latter, mainly given that most catchment storage related studies have been conducted in single catchments and using only one of the aforementioned storage quantification methods. Indeed, only few currently published studies have conducted intercomparisons of storage estimations among several catchments. Some work has shown that soils and soil drainability play an important role on catchment storage on Scottish peatland dominated catchments (Tetzlaff *et al.*, 2014) and Canadian boreal wetland dominated catchments (Spence *et al.*, 2011). In contrast, geology and topography have been observed to control storage dynamics in steep forested catchments with well–drained soils in Oregon, USA (McGuire *et al.*, 2005; Hale *et al.*, 2016). Bedrock geology has also been found to control catchment storage dynamics in 16 Luxembourgish catchments (Pfister *et al.*, 2017); whereas catchment elevation was

Patricio Xavier Lazo Jara

reported to control storage in 21 Alpine Swiss catchments, as elevation influences the snow versus soil water proportions contributing to storage (Staudinger *et al.*, 2017).

Despite these recent efforts aiming at understanding storage and the factors controlling its dynamics in several parts of the world, still there exist many remote and understudied regions (such as the humid tropics) where detailed WBB and TB information are usually lacking. In this study, we take advantage of a unique dataset of hydrometeorological and isotopic information collected in the period 2011–2014 in the nested system of 7 headwater Andean Páramo catchments of the Zhurucay River Ecohydrological Observatory (Mosquera *et al.*, 2015, 2016a, 2016b). WBB and TB storage estimations using these data, in combination with detailed information on the biophysical features of the landscape (e.g., soil cover, vegetation cover, geology, topography, rainfall regime) and soils' hydrophysical properties of the monitored catchments, provide a unique opportunity to investigate: what is the storage of the catchments and how such observable features might affect its dynamics at the catchment scale? As such, the objectives of this study are: 1) to quantify the *PasS* and *DynS* of the catchments at different temporal scales (event–based to few years); 2) to compare different *PasS* calculation methods in order to validate the TB *PasS* estimations; and 3) to examine whether catchment features, if any, control their *PasS* and *DynS*.

2. MATERIALS AND METHODS

2.1. Study site

The study site is the Zhurucay River Ecohydrological Observatory (ZREO), located in south Ecuador. The ZREO is situated on the western slope of the Pacific–Atlantic continental divide within the Andean Mountain range. The observatory expands over an altitude range between 3,400–3,900 m a.s.l. (Figure 1). The climate is mainly influenced by both, Atlantic and Pacific regime (Crespo *et al.*, 2011). Mean annual precipitation is 1345 mm with low yearly seasonality. Rainfall is mainly composed of drizzle year–round (Padrón *et al.*, 2015). Mean annual temperature is 6.0 °C and mean annual relative humidity is 90% at 3,780 m a.s.l. within the study site (Córdova *et al.*, 2015).

Patricio Xavier Lazo Jara
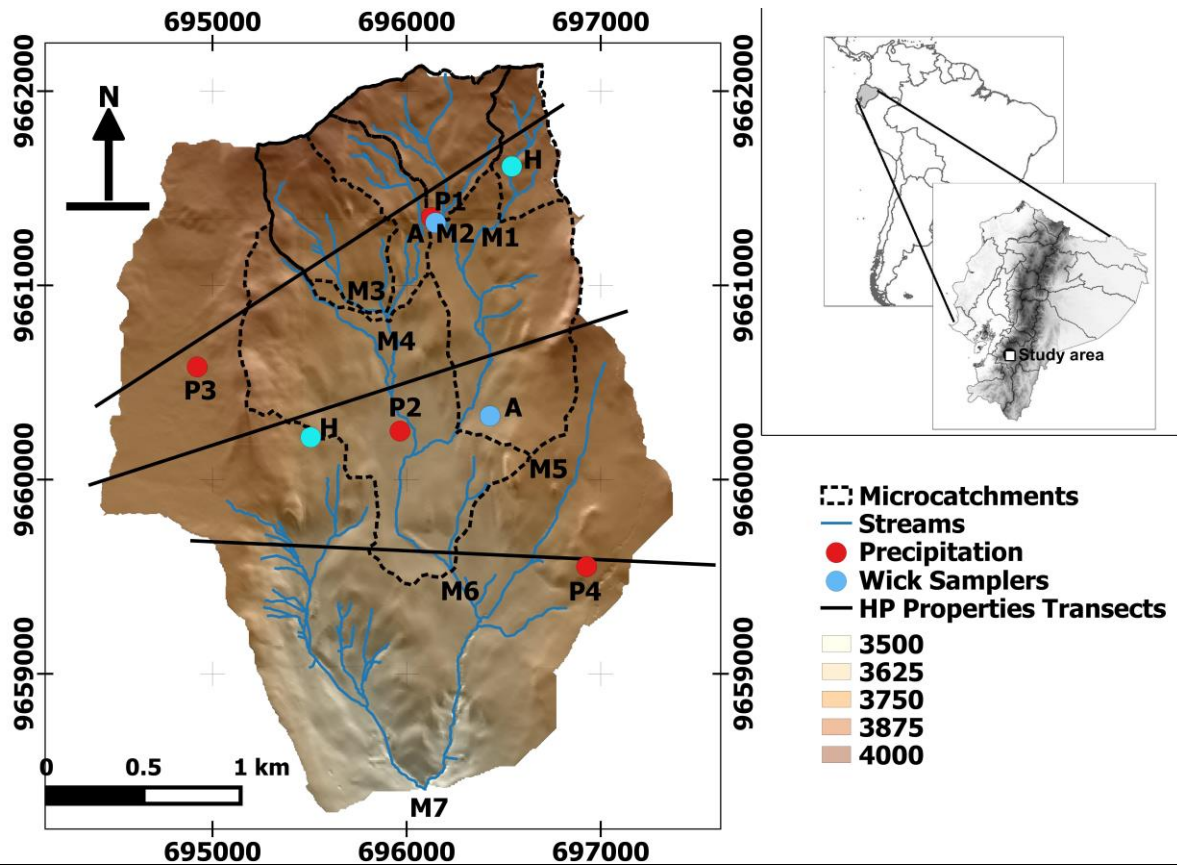
Figure 1. . Location of the study area and the isotopic monitoring network within the Zhurucay River Ecohydrological Observatory for: Streamflow (M), Precipitation (P), Andosol (A), and Histosol (H) soils. The straight black lines shown in the figure depict the transects that were used to characterized the soils' hydrophysical properties every 150 m within the catchment. *Only rainfall amount data was collected at stations P3 and P4.

The geomorphology corresponds to glaciated U–shape valleys with an average slope of 17%. Most of the land surface (69%) has slopes up to 20%, although it could reach up to 40% in some small areas (less than 5% of the total catchment area) (Table 1; Mosquera *et al.*, 2015). The geology of the observatory is composed by deposited volcanic rocks that have compacted because of the glacial activity (Coltorti and Ollier, 2000). Two geologic formations from the late Miocene period are found. The Quimsacocha formation composed by balsaltic flows with plagioclases, feldspars, and andesitic pyroclastics and the Turi formation composed by tuffaceous andesitic breccias, conglomerates, and horizontal stratified sands.

Patricio Xavier Lazo Jara

Table 1. Landscape features and hydrometric variables of the nested system of catchments of the ZREO (From Mosquera *et al.*, 2015).

Catchment	Area (km²)	Slope (%)	Distribution of soil types (%)		Vegetation Cover (%)				Geology (%)		
			Andosol	Histosol	Tussock grass	Cushion plants	Polylepis Forest	Pine Forest	Turi	Quaternary Deposits	Quimsacocha
M1	0.20	14	87	13	85	15	0	0	0	0	100
M2	0.38	24	85	15	87	13	0	0	1	33	66
M3	0.38	19	84	16	78	18	4	0	41	0	59
M4	0.65	18	80	20	79	18	3	0	48	1	50
M5	1.40	20	80	20	78	17	0	4	1	30	70
M6	3.28	18	78	22	73	24	1	2	30	20	50
M7	7.53	17	76	24	72	24	2	2	31	13	56

Catchment	Precipitation (mm y^{-1})	Total Runoff (mm y^{-1})	Runoff Coefficient	Flow rates, as frequency of non–exceedance (l s^{-1} km^{-2})						
				Qmin	Q10	Q30	Q50	Q70	Q90	Qmax
M1	1300	729	0.56	0.7	2.7	6.6	14.3	26.4	50.1	1039.0
M2	1300	720	0.55	1.2	4.8	7.9	14.9	26.7	49.0	762.9
M3	1293	841	0.65	2.3	7.3	10.8	17.7	28.1	52.4	894.2
M4	1294	809	0.62	4.2	6.2	9.8	16.6	27.3	52.1	741.2
M5	1267	766	0.60	1.5	4.1	8.3	15.3	26.9	50.8	905.7
M6	1254	786	0.63	1.2	3.7	8.2	15.9	27.5	53.2	930.4
M7	1277	864	0.68	1.9	4.0	8.7	15.2	29.2	60.8	777.9

The soils at the study area mainly correspond to Andosols and Histosols. These soils were formed by the accumulation of volcanic ashes over the valley bottoms and low gradient slopes. As a result of the cold–humid environmental conditions, they are black, humic, and acid soils rich in organic matter with high water storage capacity (Quichimbo et al., 2012). Andosols cover 76% of the observatory and are mainly found on the hillslopes; while the Histosols cover the remaining 24% and are normally found in flat areas at valley bottoms (Mosquera *et al.*, 2015). Vegetation at the study site is composed by Cushion plants (*Plantago rigida, Xenophyllum humile, Azorella spp.*) mainly covering the Histosols and tussock grass (*Calamagrostis sp.*) mainly covering the Andosols. The combination of cushion plant vegetation unit and Histosols' pedogolical unit is hereafter referred as wetlands.

2.2. Hydrometric information

Discharge, precipitation amount, and meteorological variables were continuously recorded since November 2011 to November 2014. Discharge was measured in six nested catchments using V–notch weirs and at the outlet of the catchment using a rectangular weir. The weirs were instrumented with

Schlumberger pressure transducers with a precision of ±5 mm. Water levels were recorded at a 5–minute resolution and transformed into discharge using the Kindsvater–Shen relationship. Discharge equations were calibrated using constant rate salt dissolution measurements (Moore, 2004). Precipitation was recorded using HOBO tipping bucket rain gauges with a resolution of 0.2 mm at four stations located within the catchment (Figure 1). A set of meteorological variables were also recorded from a Campbell Scientific meteorological station located next to the tipping bucket P1 (Figure 1). Temperature and relative humidity were recorded with a CS–215 combined probe protected with a radiation shield. Wind speed was recorded using a Met–One 034B Windset anemometer and solar radiation using a CS300 Apogee pyranometer. Reference Evapotranspiration (ET_o) during the study period was calculated by Córdova *et al.* (2015) at the study site using the FAO–56 Penman–Monteith equation (Allen *et al.*, 1998).

2.3. Characterization of the soils' hydrophysical properties

Soil samples were collected at 45 sampling locations separated 150 m along three transects within the study site. Samples were collected at different positions along the landscape, i.e., valley bottom, toe slope, lower slope, middle slope, upper slope, and summit (FAO, 2009; Schoeneberger *et al.*, 2012). At each sampling point and position, we characterized the soil depth, soil types, soil horizons (organic and mineral), and the thickness of each of the horizons. Two kilograms of disturbed soil and two undisturbed soil samples (using 100 cm^3 steel rings, 5 cm diameter) were collected at each sampling location and soil horizon. Upon collection, the samples were carried out to the Soil Hydrophysics Laboratory at the Univesity of Cuenca for analyzing the soil water tension–water content (θ) relationships at saturation (pF 0) and field capacity (pF 2.54). The θ at saturation was obtained via gravimetry and at field capacity via the ceramic plates system method (USDA and NRCS, 2004). The θ values are reported as volumetric moisture (mm^3 mm^{-3}).

2.4. Collection and analysis of isotopic data

Weekly water samples for Oxygen–18 (^{18}O) isotope analysis were collected for the period May 2012 – May 2014. These samples were collected in streamflow, precipitation, and soil water. Grab samples in streamflow were collected at the same stations used for measuring discharge. Water samples in precipitation were collected using two rain collectors located at 3,780 and 3,700 m a.s.l. (P1 and P2, respectively, in Figure 1). Precipitation water samples were collected from polypropylene rain collectors with a 5 mm mineral oil layer and covered with aluminum foil to reduce evaporation of the stored water. Once precipitation samples were collected, the rain collectors were cleaned, dried, and the mineral oil replaced before their re–installation.

Soil water samples were collected using wick samplers installed at four locations (2 Histosols and 2 Andosols) (Figure 1). The wick samplers were built with 9.5 mm–diameter fiberglass wicks connected to a polypropylene container of 30 x 30 cm (Boll *et al.*, 1991, 1992; Knutson *et al.*, 1993) One end of the wick was connected to the wick sampler and the other to a 1.5 L glass bottle where the soil water was collected and stored. In order to collect the mobile soil water fraction (Landon *et al.*, 1999), we applied 1 m length of suction (Holder *et al.*, 1989). The wick samplers were installed at three depths at all soil water sampling stations. In the Histosols, they were placed at 25 and 45 cm depths in the organic horizon and at 75 cm depth in the organic–mineral horizons interface. In the Andosols, they were placed at 25 and 35 cm depths in the organic horizon and at 65 cm depth in the shallowest part of the mineral horizon. The wick samplers in the Histosols were located at flat zones near the streams, whereas Andosol 1 (A1) and Andosol 2 (A2) were located at the middle and bottom parts of a hillslope. Rainfall and soil water samples were filtered using 0.45 μm filters in order to minimize organic matter contamination. The collected water samples were stored in 2 ml amber glass bottles, covered with parafilm, and kept away from sunlight to diminish fractionation by evaporation.

Patricio Xavier Lazo Jara

A cavity ring–down spectrometer (Picarro L1102–i) was used to measure the [18]O isotopic composition of the water samples with a 0.1‰ precision. Contamination of the isotopic signal was checked using ChemCorrect 1.2.0 (Picarro, 2010). This evaluation showed that only 3 soil samples (0.5% of the total) were contaminated with organic compounds. Those samples were excluded from the analysis. Isotopic concentrations are presented in the δ notation and expressed in per mill (‰) according to the Vienna Standard Mean Ocean Water (V–SMOW; Craig, 1961).

2.5. Soil water mean transit time (MTT)

Mean transit time is defined as the time it takes for a water molecule to travel subsurface in a hydrologic system (McGuire and McDonnell, 2006). That is, from the time it enters as precipitation or snow to the time it exists at an outlet point (e.g., streamflow, spring, soil wick sampler, or lysimeter). The approach used to estimate soil water MTT was based on the lumped convolution method (Maloszewski and Zuber, 1996), which assumes a steady–state condition of the flow system. Even though the steady–state assumption has been criticized as an unrealistic catchment representation in a variety of environments, the particular catchment features (i.e., relatively homogeneous soil distribution and compact geology) and low seasonal variation of hydrometeorological conditions at the ZREO, justify this assumption in our study catchment, as denoted by Mosquera *et al.* (2016b). This method transforms the input tracer signal (precipitation or snowmelt; δ_{in}) into the output tracer signal (stream, soils; δ_{out}). The input tracer concentration was volume weighted by precipitation amount to account for different recharge rates along the year, with the recharge mass variation given by the following equation:

$$\delta_{out}(t) = \frac{\int_0^\infty g(\tau) \, w(t-\tau) \, \delta_{in}(t-\tau) d\tau}{\int_0^\infty g(\tau) \, w(t-\tau) d\tau} \quad \text{(Eq. 1)}$$

where, τ is the integration variable representing the MTT of the tracer, $(t-\tau)$ is the time lag between the input and output tracer signals, $g(\tau)$ is the transit time distribution (TTD) that describes the tracer's subsurface transport, and $w(t)$ is a recharge mass variation function. The latter was applied to take into account the temporal variability in recharge rates by weighting the input isotopic composition based on precipitation amounts (McGuire and McDonnell, 2006). We tested five TTDs for the simulations: the exponential model (EM), exponential–piston flow model (EPM), the dispersion model (DM) (Małoszewski and Zuber, 1982), the gamma model (GM) (Kirchner *et al.*, 2000), and the two parallel linear reservoir model (TPLR) (Weiler *et al.*, 2003). Similarly to the findings of Mosquera *et al.* (2016b) during the evaluation of streamflow MTTs at the ZREO, the TTD that best represented the subsurface transport of water through the soils was the EM. Therefore, the soil water MTTs reported below correspond to the estimations based on this TTD.

2.6. Passive storage estimations

Passive storage is mathematically expressed as follows:

$$PasS = MTT * i \quad \text{(Eq. 2)}$$

where: i is the mean annual discharge over the period MTT was estimated for each catchment. For the nested system of catchments we estimated *PasS* based on the streamflow MTTs (in this study the values reported by Mosquera *et al.* (2016b) using the same methodology described in the section 2.5, Table 2, hereafter referred as $PasS_{(Q)}$).

We also approximated the *PasS* at the outlet of the basin (M7) based on two additional methodologies in order to examine how much of the catchments' $PasS_{(Q)}$ is represented by the soils. The first alternative approach was based on the soils' hydrophysical properties (hereafter referred as $PasS_{(HP)}$). Given the high water retention capacity of the Páramo soils and the sustained year–round rainfall at the study site (Padrón *et al.*, 2015), we assumed that their soil moisture content remains high and near saturation conditions along the year (Buytaert, 2004). Consequently, we also assumed that the contribution of the soils to the catchment *PasS* should be between the storage of the soils at saturated

Patricio Xavier Lazo Jara

conditions and above field capacity. As such, we used the θs at pF 0 (saturation) and pF 2.54 (field capacity) for each of the soils located at each of the positions along the slopes (as described in section 2.3 and shown in Figure 1), and integrated these values to the total catchment area. The integration was conducted by mapping the landscape surface that corresponded to the different positions were the hydrophysical properties of the soils were measured (i.e., valley bottom, toe slope, lower slope, middle slope, upper slope, and summit). For example, for estimating the $PasS_{(HP)}$ of the catchment at the middle of the slope, we mapped the area of the whole catchment corresponding to a slope of 32–40% and with Andosol soil type (as indicated in Table 3). We did the same for each position and soil type within the landscape where the hydrophysical soils' properties were measured. Once we classified the proportions of the landscape corresponding to each position; we used their estimated areas, θs, and soils´ horizon types and thicknesses for estimating the $PasS_{(HP)}$ at both saturation and field capacity for the catchment outlet.

The second alternative approach was based on the soil water MTT estimations (hereafter referred as $PasS_{(S)}$). In this approach, the i value in Eq. 2 was estimated using the median annual values of the ratio between the volume of water collected on the sampling bottles (as a function of the wick samplers collection area, 900 cm^2) and the time step (i.e., weekly) in which the soil samples were collected (i.e., i = Volume / time). In this way, we estimated the $PasS_{(S)}$ for each soil type at each monitoring depth.

2.7. Dynamic storage estimation

The WBB volumes of water stored in the catchments were estimated for each day during the study period as follows (e.g., Sayama *et al.*, 2011):

$$S(t) = P(t) - Q(t) - ET_a(t) \quad \text{(Eq.3)}$$

where: $S(t)$, $P(t)$, $Q(t)$ and $ET_a(t)$ are the storage volume, precipitation, discharge, and actual evapotranspiration at time t, respectively. The long–term $DynS$ (hereafter referred as $DynS_{(LT)}$) of the nested catchments was then defined as the difference between the maximum (S_{max}) and the minimum (S_{min}) daily storage volumes obtained from Eq. 3 over the period of analysis.

Actual evapotranspiration was estimated using the following equation:

$$ET_a = f * ET_o \quad \text{(Eq. 4)}$$

where: ET_o is the potential evapotranspiration, and f is a factor which is calculated as the result of the difference between P and Q divided by ET_o (i.e., $(P–Q)/ET_o$) (Staudinger *et al.*, 2017)

2.8. Runoff events selection and variables

We selected rainfall–runoff events for the analysis of the temporal variability of $DynS$ at the event scale (hereafter referred as $DynS_{(ES)}$). These events were defined as runoff response to rainfall inputs where discharge increased from below low flow values (Smakhtin, 2001) – below Q_{35} non–exceedance flow rates (determined as low flows at the ZREO, Mosquera *et al.*, 2015) – to values higher than this threshold during the duration of the events. Only events in which discharge at the end of the event returned to the discharge at the beginning of the event were considered in this study. Although rainfall–runoff events were evaluated at all catchments, only the results for the outlet of the basin (M7) are reported as similar trends for all catchments were found. Under these considerations, 42 events were selected for the analysis at M7.

For each event, we evaluated the storage–discharge hysteresis. This was conducted by visual inspection of the plots of the normalized fractional storage S_f and fractional discharge Q_f (Davies and Beven, 2015). These values are defined as the storage and discharge volumes as fractions of the

Patricio Xavier Lazo Jara

$PasS_{(Q)}$ (i.e., $S_f = S/PasS_{(Q)}$ and $Q_f = Q/PasS_{(Q)}$, respectively), where S and Q are the same as in Eq. 3 but estimated at 5–minute temporal resolution for the analysis at the event scale.

Additionally, we also estimated the cumulative Q ($Q_{(cum)}$), cumulative P ($P_{(cum)}$), cumulative ET_a ($ET_{a(cum)}$), the minimum, mean, and maximum rainfall intensity, as well as the antecedent wetness conditions of the catchment represented as the amount of antecedent precipitation over different time periods (7 and 14 days before each event) for each of the 42 events to investigate their influence on $DynS_{(ES)}$.

2.9. Statistical analysis between storage and landscape–hydrometric features

We conducted a Pearson linear correlation analysis between the estimates of $PasS_{(Q)}$ and $DynS_{(LT)}$ and different landscape features which included: catchment area, soil cover, vegetation cover, geology, and average slope of each catchment. We also conducted a linear correlation analysis between $PasS_{(Q)}$ and $DynS_{(LT)}$ with hydrometric variables that included mean annual P, mean annual Q, mean annual ET_a, runoff coefficient (Q/P), and different non–exceedance flow rates according to the catchment's flow duration curves. The biophysical and hydrometric features of the catchments were obtained from Mosquera *et al.* (2015) (Table 1).

At the event scale, linear correlation analysis was used to investigate relations between $DynS_{(ES)}$ with all the hydrometeorological variables estimated for the rainfall–runoff events. All correlations were evaluated using the determination coefficient (r^2) and their statistical significance was tested with a 90% confidence level (p–value $\leq$ 0.1) using the t–student test.

3. RESULTS

3.1. Catchments' passive and dynamic storage estimations

The $PasS_{(Q)}$ estimations of the catchments varied from 313 to 617 mm, with a value of 457 mm at the outlet of the basin (M7). The maximum values were observed at catchments M3 and M4, while the minimum value at M2 (Table 2). The variation among catchments (304 mm) was large. On the other hand, their $DynS_{(LT)}$ ranged from 29 to 35 mm, showing little differences among subcatchments (6 mm). Similarly to the $PasS_{(Q)}$, catchments M3 and M4 showed the maximum values while the minimum value corresponded to M7. The fractions of $DynS_{(LT)}$ to $PasS_{(Q)}$ varied between 6 and 10% among the catchments (Table 2).

Table 2. Streamflow TB Passive ($PasS_{(Q)}$) and long–term Dynamic Storage ($DynS_{(LT)}$) estimations for the nested system of catchments at the ZREO using data collected in the period Nov 2011–Nov 2014. *Catchments' MTTs estimations were obtained from Mosquera *et al*., 2016b.

Catchment	Streamflow MTTs* (days)	Passive Storage (mm)	Dynamic Storage (mm)	Dynamic Storage/Passive storage (%)
M1	194 (171 – 227)	394 (341 – 453)	34 (31 – 37)	9
M2	156 (137 – 186)	313 (270 – 361)	31 (28 – 34)	10
M3	264 (232 – 310)	617 (534 – 714)	35 (32 – 38)	6
M4	240 (212 – 280)	539 (470 – 621)	33 (31 – 36)	6
M5	188 (165 – 219)	400 (346 – 460)	32 (29 – 35)	8
M6	188 (164 – 220)	411 (353 – 474)	31 (29 – 34)	8
M7	191 (167 – 224)	457 (395 – 530)	29 (26 – 32)	6

Patricio Xavier Lazo Jara

In regards to the daily temporal variability of the WBB catchments' water storage volume (Figure 2), although the system showed a very flashy response of storage volume to precipitation, it normally returned to a stability condition with $S(t)$ around 0 mm day^{-1}. Also, although the occurrence of negative ($S(t) < 0$ mm day^{-1}; when the system loses or discharges higher amounts of water than the inputs) and positive values ($S(t) > 0$ mm day^{-1}; when the system gains or receives higher amounts of water than it discharges) were almost the same (53 and 47%, respectively); the system tended to be recharged with higher amounts of water (i.e., the absolute values of $S(t)$ were higher) than when it discharged (i.e., the absolute values of $S(t)$ were lower) (Figure 2). The latter coinciding with the most humid periods between March–May for every year during the monitoring period (Figure 2).
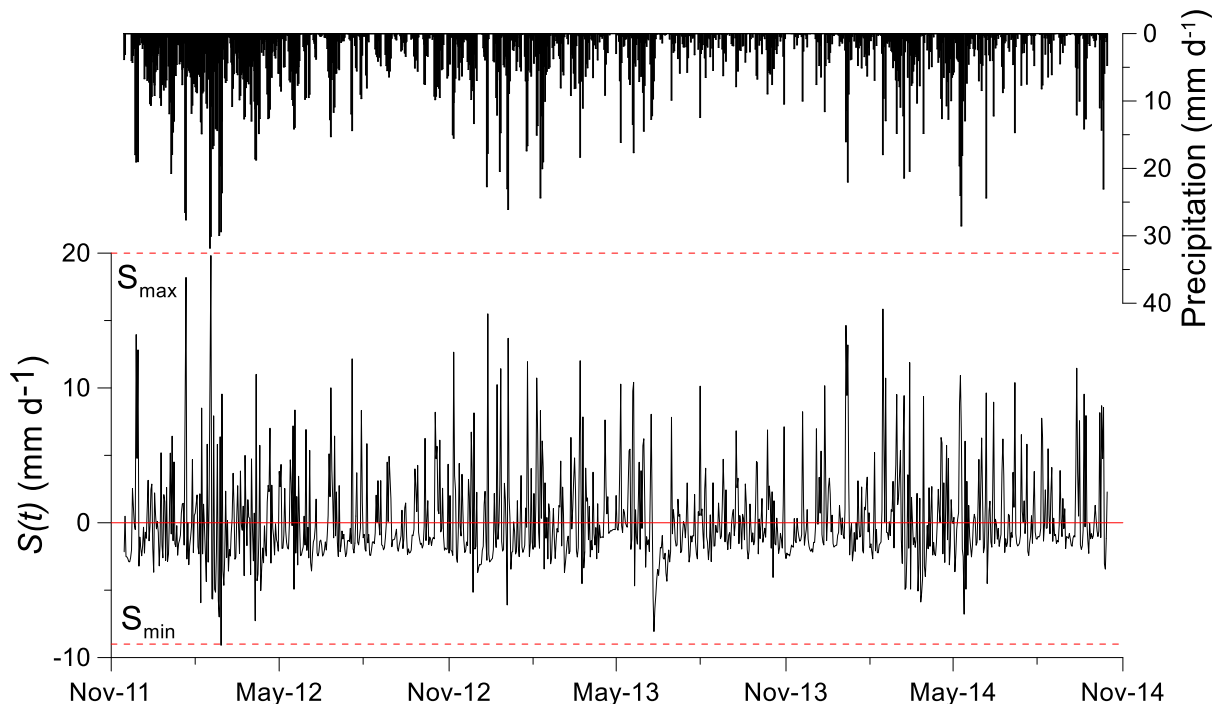

Figure 2. Daily precipitation and change of storage volume $S(t)$ at the outlet of the catchment (M7) for the period Nov 2011–Nov 2014. Continuous red line represent $S = 0$ mm day^{-1} while dashed red lines represents the maximum (S_{max}) and minimum (S_{min}) storage volumes which were used to estimate the long–term dynamic storage ($DynS_{(LT)} = S_{max} - S_{min}$).

3.2. Hydrophysical soil properties based catchment passive storage estimations

The hydrophysical properties (i.e., θ at pFs 0 and 2.54) of the soils located at the different landscape positions and their areal extent within the ZREO are presented in Table 3. The Histosols were only found at the valley bottom and toe slope positions. Their average thickness was 700 mm for the organic horizon and 500 mm for the mineral horizons. Histosols were normally found in low relief areas with slopes between 1–15% and covered 1.81 km^2 (24% of the total catchment area). They presented the highest θs at saturation (pF 0) for the organic (0.89–0.90 mm^3 mm^{-3}) and the mineral horizon (0.65 cm^3 cm^{-3}). Histosols also presented the highest θs at field capacity (pF 2.54) for the mineral horizon (0.54 cm^3 cm^{-3}), but among the lowest for the organic horizon (0.62–0.63 mm^3 mm^{-3}). The Andosols on the other hand, were found from the toe slope to the summit positions along the hillslopes. Their thickness was more variable than for the Histosols, and ranged between 300–400 mm for the organic horizon and 200–300 mm for the mineral horizon. They were found along the whole range of relief areas (1 – >56%) and covered 5.72 km^2 (76% of the total catchment area). The θ values at saturation of the organic horizon of the Andosols (0.72–0.83 mm^3 mm^{-3}) were more variable than those at their mineral horizon (0.53–0.56 cm^3 cm^{-3}). For both horizons, these values were lower than

Patricio Xavier Lazo Jara

for the Histosols. Their θ values at field capacity for the organic horizon of these soils (0.62–0.69 mm^3 mm^{-3}) were more variable and higher than those for their mineral horizons (0.46–0.50 mm^3 mm^{-3}).

Table 3. Hydrophysical properties for each soil type, horizon, and position within the ZREO and passive storage estimations based on these properties ($PasS_{(HP)}$) in relation to the areal extent of each of them with respect to the total basin area, M7. $PasS_{(HP)}$ estimates were calculated at field capacity (FC) and saturation (Sat) conditions.

	Position on the hillslope	Soil Type	Slope	Soil depth	Area	pF 2.3	pF 0	Soil $PasS_{(HP)}$ Capacity		Total	
								FC	Sat	FC	Sat
			(%)	(mm)	(km^2)	(mm^3/mm^3)	(mm^3/mm^3)	(mm)	(mm)	(mm)	(mm)
Organic Horizon	Valley bottom	Histosol	1–5	700	0.07	0.62	0.90	17	24	441	623
	Toe slope	Histosol	5–15	700	1.74	0.63	0.89	424	599		
		Andosol		400	0.26	0.62	0.72	11	13		
	Lower slope	Andosol	15–32	300	1.66	0.67	0.83	58	72		
	Middle slope	Andosol	32–40	350	2.51	0.69	0.76	106	117	230	264
	Upper slope	Andosol	40–56	380	0.59	0.65	0.74	25	29		
		Andosol	>56	380	0.42	0.65	0.74	18	21		
	Summit	Andosol	1–5	335	0.28	0.65	0.73	11	12		
Mineral Horizon	Valley bottom	Histosol	1–5	500	0.07	0.54	0.65	10	13	270	325
	Toe slope	Histosol	5–15	500	1.74	0.54	0.65	260	312		
	Toe slope	Andosol		300	0.26	0.50	0.53	7	7		
	Lower slope	Andosol	15–32	300	1.66	0.46	0.56	40	49		
	Middle slope	Andosol	32–40	300	2.51	0.46	0.56	61	74	131	156
	Upper slope	Andosol	40–56	200	0.59	0.46	0.53	9	11		
		Andosol	>56	200	0.42	0.46	0.53	7	8		
	Summit	Andosol	1–5	310	0.28	0.46	0.53	7	8		

The $PasS_{(HP)}$ was variable among the different soil types and horizons at the different positions in the landscape (Table 3). The $PasS_{(HP)}$ estimations using these soil properties and the spatial distribution and thickness of each soil horizon showed that the Histosols stored a higher amount of water (711 mm at FC and 948 mm at saturation) than the Andosols (361 mm at FC and 420 mm at saturation) (Table 4). Integrating these $PasS_{(HP)}$ values to the catchment scale using the areal proportions of the catchment covered by each soil type, the $PasS_{(HP)}$ at the outlet of the basin (M7) were 445 mm at field capacity and 547 mm at saturation (Table 4).

Patricio Xavier Lazo Jara

Table 4. Passive storage estimations based on the soils' hydrophysical properties ($PasS_{(HP)}$) at field capacity (FC) and saturation (Sat) for the organic and mineral horizon of the Andosols and Histosols and the integration of this storage to the catchment outlet, M7, based on the areal extent of each soil type within the ZREO.

	FC		Sat	
	(mm)		(mm)	
	Histosol	Andosol	Histosol	Andosol
Organic Horizon	441	230	623	264
Mineral Horizon	270	131	325	156
Soil $PasS_{(HP)}$	711	361	948	420
Soil area percentage (%)	24	76	24	76
Catchment $PasS_{(HP)}$	445		547	

3.3. Soil water MTT based catchment passive storage estimations

Soil water MTTs for Andosols and Histosols at the three monitored depths are reported in Table 5. The MTTs in both soil types increased with depth. MTTs in the Andosols were 35 and 48 days for the shallower organic horizons and 144 days for the organic–mineral horizons interface. MTTs in the Histosols were longer than in the Andosols, with values of 212 and 292 days for the shallower organic horizons and 338 days for the organic–mineral horizon interface. With these MTT values we estimated the $PasS_{(S)}$ for each soil type at each monitoring depth (Table 5). Andosols showed $PasS_{(S)}$ values ranging between 14 to 49 mm, with the highest contribution from the mineral horizon (at 65 cm depth). Histosols showed higher $PasS_{(S)}$ values, and similarly to the soil water MTTs, these values increased with depth. $PasS_{(S)}$ was 191 and 263 mm at the shallower organic horizons and 304 mm at the organic–mineral horizons interface (at 65 cm depth). Based on the $PasS_{(S)}$ values at each soil type and horizon, the water storage was 97 mm for the Andosols and 759 mm for the Histosols.

Table 5. Soil water discharge (i), soil water MTTs and soil water TB passive storage ($PasS_{(S)}$) for the monitored soil types and depths using data collected in the period Nov 2011–Nov 2014. Values in parenthesis correspond to the 5% and 95% confidence intervals.

Soils	i (mm/day)	MTT (days)	$PasS_{(S)}$ (mm)
Andosol–25	0.95	35 (26 – 48)	33 (25 – 45)
Andosol–35	0.30	48 (39 – 59)	14 (11 – 17)
Andosol–65	0.34	144 (119 – 166)	49 (41 – 57)
Histosol–25	0.90	212 (187 – 247)	191 (168 – 222)
Histosol–45	0.90	292 (263 – 331)	263 (236 – 298)
Histosol–70	0.90	338 (298 – 394)	304 (268 – 355)

3.4. Temporal variation of dynamic storage at the event scale

The 42 rainfall–runoff events selected for the analysis represented a wide variety of hydrometeorologic conditions during the study period. The $P_{(cum)}$ at the end of the events ranged between 0.2–56.0 mm; with $Q_{(cum)}$ varying between 1.2–52.8 mm, and $ET_{a(cum)}$ between 0.1–16.6 mm. The $DynS_{(ES)}$ during the events were 0.07–1.91 mm. In addition, maximum, mean, and minimum P

Patricio Xavier Lazo Jara

intensities during the events were in the range of 0.6–22.3 mm h^{-1}, 0.1–5.4 mm h^{-1}, and 0 to 1.1 mm h^{-1}, respectively. Antecedent P for 7 and 14 days prior to the start of the events ranged between 2.6–68.5 mm and 15.8–113.3 mm.

The temporal variability of S_f during the events was similar for all catchments and a representative one at the outlet of the catchment (M7) is shown in Figure 3. The event had a total duration of 50 hours and during this period $P_{(cum)}$ and $Q_{(cum)}$ were 32.2 and 32.3, respectively. Figure 3 shows that at the beginning of the event (t_0), the system starts at relatively stable conditions (i.e., $S_f = 0$; not storing, nor releasing water). During the first 17.7 hours (t_1), 82% of the $P_{(cum)}$ entered to the system. During this period, corresponding to the rising limb of the Q hydrograph (black line in Figure 3a), the catchment did not only release water via Q in response to the P inputs (black line in Figure 3c), but also was dynamically recharged ($S_f > 0$ mm) in a non–linear fashion (black line in Figure 3b). From then on, once rainfall intensity decreased, the system continued to change from a recharge state at a lower rate to a releasing water state until t_2 at around 18.3 hr. This water loss from the catchment took place in a mostly linear fashion and in such a flashy way, that the peak of the hydrograph (t_2) was actually caused by the loss of moisture from the recharged system rather than from precipitation (i.e. the black line in the negative region of the S_f during the t_1–t_2 period in Figure 3b). After this time, when rainfall almost completely ceased, the release of water from the system was almost sustained until t_3 (18.6 hr), when the system started to be linearly discharged in a relatively constant but rapid manner (grey line in Figure 3b). This effect thus causing a very steep falling limb of the Q hydrograph at the end of the event (grey line in Figure 3a), when the system again reached a stability condition ($S_f \approx 0$ mm) at the end of the event, 50 hours after its beginning (t_f). The S_f dynamics at the event scale formed an anticlockwise hysteretic loop. All of the monitored events at all catchments followed the same hysteretic direction.
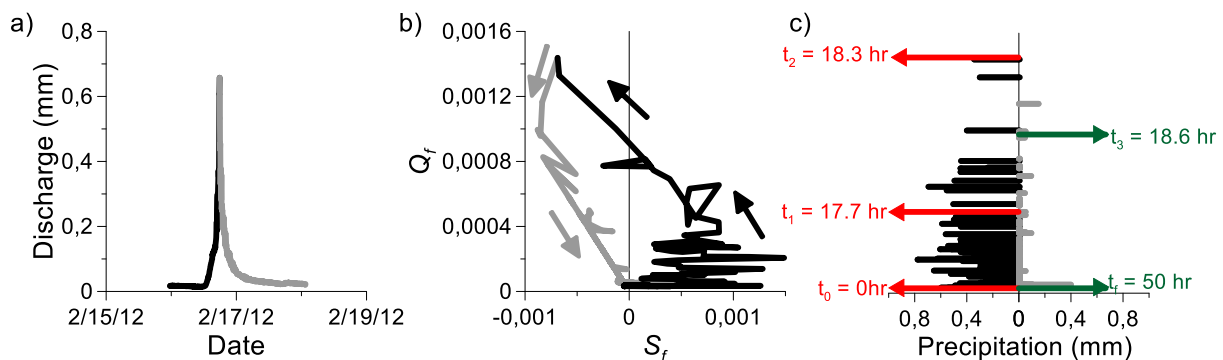

Figure 3. a) Discharge hydrograph; b) evolution of the normalized fractional storage volume S_f; and c) rainfall intensity during a representative rainfall–runoff event at the study site. The data correspond to an event monitored at the outlet of the basin on February 16th, 2012. Black lines correspond to the rising limb and grey lines to the recession limb of the discharge hydrograph during the event. The red lines in the subplot c) represent the times during the evolution of the rising limb of the hydrograph in the subplot a); whereas the green lines represent the evolution of the hydrograph during the recession limb of the hydrograph.

3.5. Relations between storage metrics and landscape features and hydrologic variables

The $PasS_{(Q)}$ for our nested catchments was significantly positively correlated with mean annual Q ($r^2 = 0.73$, p = 0.07), runoff coefficient ($r^2 = 0.75$, p = 0.06), and high flows represented by the Q_{90} non–exceedance flows ($r^2 = 0.67$, p = 0.09) (Table 6). With regards to the landscape features, $PasS_{(Q)}$ was also significantly positively correlated with the cushion plants vegetation cover ($r^2 = 0.68$, p = 0.08) and negatively correlated with the tussock grass vegetation cover ($r^2 = 0.73$, p = 0.07) (Figure 4). Even though the areal proportion of soils (Histosols and Andosols) and vegetation (cushion plants and tussock grass) cover are highly correlated at the ZREO, respectively (Mosquera *et al.*, 2016a), and the correlation between $PasS_{(Q)}$ and the soils follows the same trend that their related vegetal cover (i.e.,

Patricio Xavier Lazo Jara

positive for the Histosols and negative for the Andosols), this correlations were not statistically significant ($r^2 < 0.55$, $p > 0.15$). Neverteless, given the fact that Histosols and Andosols underlies cushion plants and tussock grass respectively, the latter could be as a result of the lesser precision of the soils' map compared with the vegetation's map.

Table 6. Pearson correlations (r^2) between the streamflow TB passive storage ($PasS_{(Q)}$) of the catchments with landscape features and hydrologic variables. Values in bold represent the correlations with a confidence level of 90% ($p \leq 0.10$). +/– values represents a positive or negative correlation between the variables, repectively. Q_{xx} represents the flow rates, as frequency of non–exceedance, where xx shows the non– exceedance rate.

|	Variable name	$PasS_{(Q)}$
Hydrologic variables	Dynamic Storage (mm)	–0.20
	Passive Storage	**1.00**
	Mean Annual Precipitation	–0.30
	Mean Annual Discharge	**0.73**
	Runoff Coefficient	**0.75**
	Q_{min}	0.24
	Q_{10}	–0.18
	Q_{30}	0.10
	Q_{50}	0.13
	Q_{70}	0.55
	Q_{90}	**0.67**
	Q_{max}	0.03
Landscape features	Area (km²)	0.61
	Slope (%)	–0.45
	Andosols (% of total area)	–0.56
	Histosols (% of total area)	0.51
	Tussock Grass (% of total area)	**–0.73**
	Cushion plants (% of total area)	**0.68**
	Turi Formation (% of total area)	0.48
	Quaternary Deposits (% of total area)	–0.28
	Quimsacocha Formation (% of total area)	–0.05

Patricio Xavier Lazo Jara
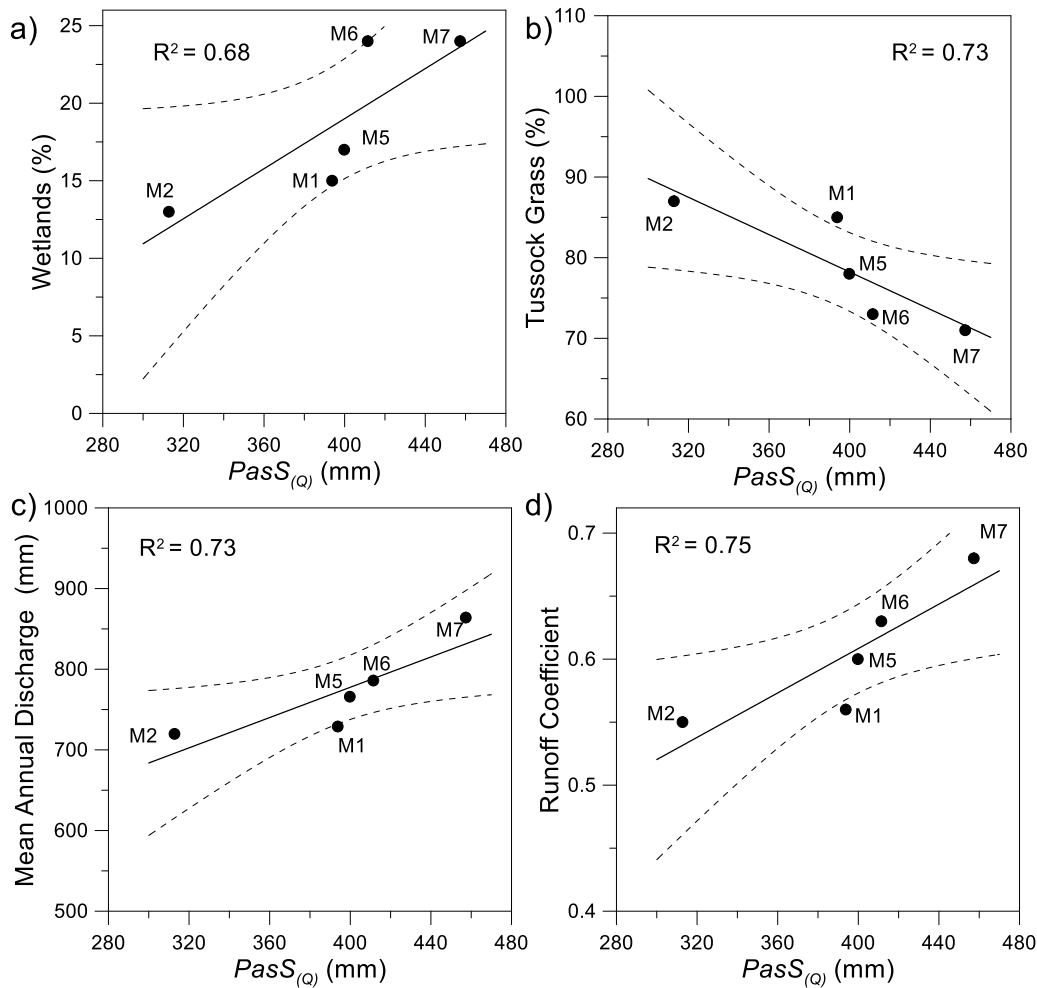
Figure 4. Correlations between the streamflow TB passive storage ($PasS_{(Q)}$) of the nested system of catchments with a) cushion plants, b) tussock grass, c) mean annual discharge, and d) runoff coefficient. Vegetation is expressed as the percentage the areal extent of each vegetation type to the total area of each catchment. Dashed lines represents the 95% and the 5% confidence intervals.

For the $DynS_{(LT)}$ estimations calculated from the daily WB analysis, we found statistically significant correlations with landscape and hydrologic variables. However, due to the small range of variation of $DynS_{(LT)}$ among catchments (only 6 mm, Table 2), we acknowledge that these correlations may not be causal and thus do not report them. On the short term, when analyzing correlation between hydrometeorological variables and the $DynS_{(ES)}$ during the events monitored at the outlet of the basin, M7, we identified non–significant correlations between this storage metric and most hydrometeorological variables ($r^2 \leq 0.30$). These variables included the $P_{(cum)}$, $Q_{(cum)}$, $ET_{a(cum)}$, mean and minimum P intensities, and 7 and 14 days accumulated antecedent P. The only strong correlation found was between the $DynS_{(ES)}$ and the maximum P intensity during the events ($r^2 = 0.91$, p < 0.0001, Figure 5).
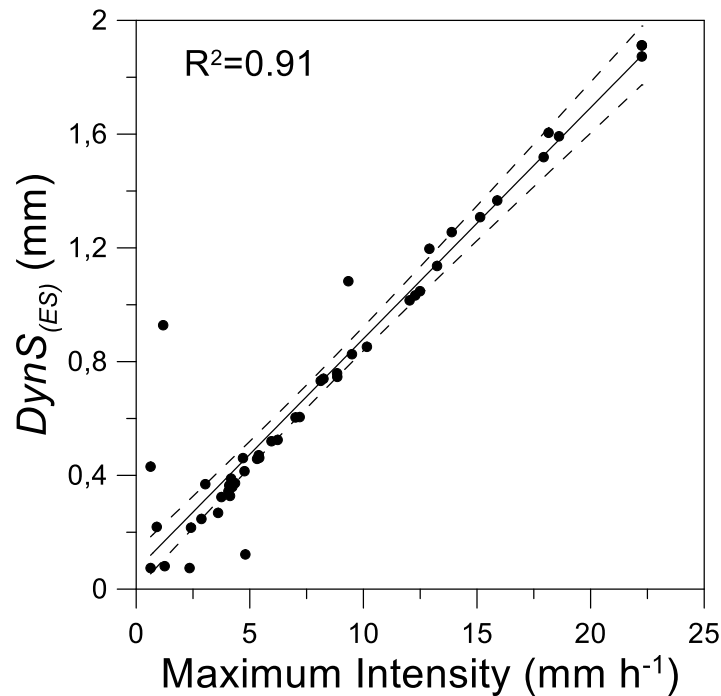
Patricio Xavier Lazo Jara

Figure 5. Correlation between the event scale dynamic storage ($DynS_{(ES)}$) and maximum P intensity during the runoff events at the outlet of the basin, M7. Dashed lines represents the 95% and 5% confidence intervals.

4. DISCUSSION

4.1. Catchments' passive water storage

Our storage evaluation using the combination of hydrometric, isotopic, and hydrophysical soil properties data in the nested system of catchments of the ZREO yielded valuable insights into the water passive and dynamic storage of the páramo.

Our estimated $PasS_{(Q)}$ values at the ZREO (313–617 mm, Table 2) are similar to those reported by Bishop *et al.* (2011) at the Gardsjön catchment in Sweden (300 mm) and Soulsby *et al.* (2009, 2011) in a group of montane Scottish catchments (265 to 688 mm). These authors attributed these relatively small storage values to the retention of water in the relatively shallow (< 2 m) peat type soils with little deeply sourced water contributions from groundwater storage. On the contrary, our estimates are low in relation to those reported by Amvrosiadi *et al.* (2017) on a peat dominated catchment in North Sweden (1189–1485 mm), Birkel *et al.* (2011) in the peat dominated Girnock catchment in the Scottish highlands (about 10000 mm), and Staudinger *et al.* (2017) in a group of catchments with different land covers (e.g., pasture, grasslands, and forests) in a gradient between the Swiss plateau and alpine regions (> 5000 mm). Despite the differences in catchment features (e.g., precipitation seasonality, land cover, soil type and depth) among the study sites investigated by these authors, they all attributed these high $PasS_{(Q)}$ estimates to water storage in deep groundwater reservoirs, i.e., the highly fractured and permeable parental material (Pfister *et al.*, 2017). At the ZREO, prior research has shown that water stored in the peatland type Histosol soils (i.e., wetlands) controls runoff generation (Mosquera *et al.*, 2015; Correa *et al.*, 2016). In addition, other studies have also shown that water originated from these wetlands is the main contributor to runoff year–round and that deeply sourced groundwater contributions to runoff are minimal (Mosquera *et al.*, 2016a; Correa *et al.*, 2017). Our $PasS_{(Q)}$ estimates, similar to those in catchments with low groundwater storage availability and much lower than those in catchments with highly fractured geology, evidence that these wetlands do not only control water production at the ZREO, but also the catchment's water storage capacity.

It is worth highlighting that two of the upper catchments (M3 and M4, Figure 1) showed the highest $PasS_{(Q)}$ (617 and 539 mm, respectively) among all monitored catchments within the ZREO. Also,

Patricio Xavier Lazo Jara

PasS(Q) of catchment M3 almost doubled that of M2 (Table 2), even when these two catchments have the same drainage areas. Similar findings have been reported by Birkel *et al.* (2011) and Soulsby *et al.* (2011) for a group of montane Scottish catchments with similar soil conditions and spatial distribution than in our páramo monitoring site. These authors found that catchments with fractured and permeable geology showed much higher *PasS(Q)* than catchments with little weathered and impermeable bedrock. At the ZREO, catchments M3 and M4 have also shown the longest streamflow MTTs (Mosquera *et al.*, 2016b) and the highest baseflows (Mosquera *et al.*, 2015) among the monitored catchments as a result of a shallow spring water contribution to runoff (i.e., from the weathered mineral horizon or the fractured shallow bedrock) (Correa *et al.*, 2017). Altogether, these findings evidence that even when the hydrology of the ZREO is in general controlled by water flowing in the shallower organic horizon of the páramo soils (Mosquera *et al.*, 2016a; Correa *et al.*, 2017), it is feasible that in the presence of a fractured parental material in other páramo catchments in the Andean region, their *PasS(Q)* could be much higher than that estimated at the ZREO outlet (M7, 457 mm).

Regarding the application of different methods for estimating catchments' *PasS* capacity, past investigations have yielded differing results (e.g., Brauer *et al.*, 2013; Staudinger *et al.*, 2017b). For instance, at the Girnock catchment in the Scottish highlands, several methods used to estimate the catchment's *PasS* yielded different results. These methods included the streamflow MTT based (*PasS(Q)*) (Soulsby *et al.*, 2009), a combination of distributed soil moisture and groundwater measurements and hydrologic modelling (van Huijgevoort *et al.*, 2016), bedrock geophysical surveys (Tetzlaff *et al.*, 2015b), and tracer–based hydrologic modelling (Birkel *et al.*, 2011), with the estimated *PasS* values yielded amongst these methods varying within two orders of magnitude. For this reason, we further evaluated how our *PasS(Q)* estimations compared to those based on the monitoring of the soils' hydrophysical properties (*PasS(HP)*) and soil water MTTs (*PasS(S)*).

The *PasS(HP)* estimates for the catchment outlet (M7) at field capacity and saturation (445 and 547 mm, respectively, Table 4) showed a remarkable agreement with respect to the *PasS(Q)* estimate (457 mm, Table 2). With respect to the *PasS* estimations based on the soil water MTTs (*PasS(S)*), due to the landscape configuration, the isotopic signal of the water from the Andosols draining down the hillslopes is already mixed at the valley bottom wetlands (Tetzlaff *et al.*, 2014; Mosquera *et al.*, 2016a), and as a result, the storage estimations from the Histosols account for the Andosols storage. The sum of the *PasS(S)* estimations at the organic horizons of the Histosols (i.e., at 25 and 45cm depth), which resulted in a total PasS of 454 mm (Table 5), was also very similar to the *PasS(Q)* estimation. These findings evidence that *PasS(Q)* provides accurate estimates of the total catchment *PasS* and that virtually the totality of the catchment water storage capacity of the ZREO outlet is stored in the páramo soils. Thus, these results provide further evidence that overall, the contributions from deep groundwater sources to runoff are minimal, as has been hypothesized in past studies at the ZREO (Mosquera *et al.*, 2016a, 2016b). These findings also evidence that the tracer signals from different parts of the catchments become well mixed within the valley bottom wetlands (Mosquera *et al.*, 2016b) and that the integration of these signals provides accurate estimates of catchment passive storage.

In this sense, it is worth noting that even though the streamflow based MTT method for estimating passive storage (*PasS(Q)*) has been widely applied in past investigations (e.g., Soulsby *et al.*, 2009; Mcnamara *et al.*, 2011; Tetzlaff *et al.*, 2015b; Hale *et al.*, 2016; Staudinger *et al.*, 2017), the accuracy of this method has been difficult to evaluate due the unobservable nature of large groundwater contributions to *PasS*. In these sense, the ZREO hydrologic conditions, i.e., a system whose hydrological behavior is dominated by shallow subsurface flow of water stored and resealed from the little developed soils with little shallow groundwater contributions (Mosquera *et al.*, 2016a, 2016b; Correa *et al.*, 2017), become ideal for investigating the accuracy of the *PasS(Q)* method. Given that the *PasS(Q)* estimations for the outlet of the catchment lie within those yielded by the potential storage of the soils (i.e., the *PasS(HP)* estimations at saturation and field capacity), our results evidence that this method yields accurate catchment *PasS* estimations.

Moreover, these results indicate that through the combined application of both these methods, one could indirectly obtain estimations of groundwater contributions that to date, are still difficult to quantify in the field or are estimated with high uncertainty using hydrologic modelling methods (e.g.,

Patricio Xavier Lazo Jara

Birkel *et al.*, 2011; Tetzlaff *et al.*, 2014, 2015a; van Huijgevoort *et al.*, 2016). For example, for catchment M3, which is influenced by the additional contribution of water from a shallow spring source to discharge, $PasS_{(HP)}$ estimations ranged between 399 and 472 mm at field capacity and saturation, respectively. As the $PasS_{(Q)}$ for this catchment was 617 mm, and assuming that the potential water storage capacity of the soils in this catchment is at saturation, it can be assumed that the extra storage capacity provided by this catchment (i.e., the storage added by the additional spring water contribution) is the difference between the *PasS* estimates yielded by these methods, i.e., about 145 mm. These results evidence the usefulness of both the $PasS_{(Q)}$ and $PasS_{(HP)}$ methods to provide indirect *PasS* groundwater estimations in catchments' at other environments.

4.2. Catchments' dynamic water storage

The dynamics of the daily water storage volumes ($S(t)$) mobilized into or out of the ZREO hydrologic system revealed a fast system's response to precipitation inputs with positive (i.e., recharge) and negative (i.e., discharge) values oscillating around an stability values of zero during the monitoring period (Figure 2). This effect can be likely attributed to the local precipitation, soil hydrophysical properties, and atmospheric conditions at the ZREO. The rapid recharge of storage volumes likely occurs as a result of the input of low intensity precipitation (Padrón *et al.*, 2015) that recharges the near saturated Histosol soils (Mosquera *et al.*, 2016a) during rainfall events. On the other hand, as precipitation inputs cease, the fast movement of water within the shallowest organic horizon of the páramo soils can cause a rapid discharge from the Histosols water storage. Additionally, the maintenance of the near saturated equilibrium conditions of these soils is likely caused by the high year–round relative humidity (Córdova *et al.*, 2015) that helps reduce water losses due to evapotranspiration (Kettridge and Waddington, 2014; Sprenger *et al.*, 2017; Tunaley *et al.*, 2017). Effects that were enhanced during the wetter periods (i.e. March to May, when precipitation is of higher intensity). During these periods, higher precipitation amount inputs caused a faster recharge/discharge response most likely due to the rapid movement of water via subsurface later flow within the shallow organic horizon of the hillslope soils that push out the water held at the riparian wetlands (Mosquera *et al.*, 2016a; Correa *et al.*, 2017). An effect that in turn can increase the discharge contributing areas (Nippgen et al., 2015; Birkel and Soulsby, 2016) and lead to rapid changes on the storage volumes.

In regards to the catchments *DynS* in the long term, $DynS_{(LT)}$ values (29 – 35 mm, Table 2) for all the catchments at the ZREO were low compared with those reported by Peters and Aulenbach (2011) (40 – 70mm), Buttle (2016) (30 – 77 mm), and Pfister *et al.* (2017) (107 – 373mm) at other ecosystems with more drainable soils than those of the páramo. On the other hand, Staudinger *et al.* (2017) found a wider range of values in Swiss pre–alpine and alpine catchments (12 – 974mm), where catchments with similar values than the ZREO were rainfall–dominated ecosystems and presented relatively small groundwater contributions. Soulsby *et al.* (2011) reported $DynS_{(LT)}$ values ranging between 2–36 mm in a group of montane Scottish catchments with similar pedological and land cover conditions than at the ZREO. These authors concluded that values close to 36 mm corresponded to catchments with relatively compacted geology, whereas values close to 2 mm corresponded to catchments with high groundwater contributions (i.e., fractured parental material). In addition, even though the porosity and saturated hydraulic conductivity of the Histosols are relatively high in comparison to the Andosols at the ZREO, because the presence of the former is almost exclusively restricted to flat areas with low hydraulic gradients (i.e., valley bottoms and flat hilltops), their water movement is reduced and mostly restricted to the shallowly rooted organic horizons (Mosquera *et al.*, 2016a; Correa *et al.*, 2017). In this sense, our relatively small $DynS_{(LT)}$ estimations indicate that the little available storage from the shallow organic horizon of the Histosol soils that are near saturation along the year (Mosquera *et al.*, 2016a), allow for a small proportion, i.e., the remaining storage until the Histosols become saturated, to be hydrologically active during runoff generation. These findings are supported by the estimated $DynS_{(LT)}$ to $PasS_{(Q)}$ ratios of the ZREO. These ratios also depicted that only a relatively small proportion of the water stored and available for mixing within the catchment is hydrologically active

Patricio Xavier Lazo Jara

(i.e., 6 to 10% is active in the water balance, Table 2). These findings likely explain the rapid changes in daily $S(t)$ volumes (Figure 2) described above and the flashy discharge response to precipitation previously reported at the ZREO (Mosquera *et al.*, 2015, 2016b).

The anticlockwise hysteretic–loop pattern between the normalized fractional storage (S_f) and the normalized fractional discharge (Q_f) (Figure 3) identified at the event scale has also been determined by field observations (e.g., Botter *et al.*, 2009; Creutzfeldt *et al.*, 2014; Beven and Davies, 2015; Hailegeorgis *et al.*, 2016) and modelling (e.g., Kirchner, 2009; Davies and Beven, 2015) at other catchments. Direction that has proven to depend on different climatic, topographic, and parental material catchment characteristics (Sproles *et al.*, 2015). At the ZREO, the observed anticlockwise is likely explained by the combined effect of the Histosols (wetlands) high water retention capacity and the year–round input of low intensity precipitation. In effect, this trend suggests that when water enters the system via precipitation at the beginning of the event, it initially infills the relatively little available soils' water storage reservoir before effective precipitation is released to the streams. Then, once a certain threshold storage that depends on the antecedent moisture conditions is reached (Mosquera *et al.*, 2016a), the soils start releasing water to streams (black lines in Figure 3a and 3b). Once precipitation ceases, the moisture gained by the soils allows for a sustained stormflow generation until the end of the event (grey line in Figure 3a and 3b), when the system returns to an stability condition (i.e., $S_f \approx 0$) because of the high water retention capacity of the soils, as has been reported by Fovet *et al.* (2015) in poorly drained riparian zones at a headwater catchment in France. The consistent anticlockwise direction observed during all monitored events at all catchments further evidences the importance of the riparian Histosols in streamflow generation at the ZREO (Mosquera *et al.*, 2016a; Correa *et al.*, 2017).

4.3. Factors controlling catchment storage

- ### Soils, vegetation, and topographic controls on passive storage

Past research at the ZREO has shown the importance of Histosol soils and wetlands' vegetation cover on the catchments' water production (Mosquera *et al.*, 2015). The high correlation between $PasS_{(Q)}$ and the wetlands cover (i.e., Histosols + cushion plants) of our nested system of catchments (Table 6, Figure 4) suggests that this soil type also influences the catchments' available storage for mixing. Similar hydrologic dependence on wetlands storage has been reported at the Scottish Highlands (e.g., Birkel *et al.*, 2011; Tetzlaff *et al.*, 2014; Geris *et al.*, 2015a, 2015b, 2017). In addition, these findings also confirm that for catchments with low groundwater contribution, the totality of $PasS_{(Q)}$ depends on their areal proportion of wetlands.–Additionally, the strong correlation between $PasS_{(Q)}$ with the catchments' mean annual discharge and runoff coefficients ($r^2 > 0.73$, Table 6), further evidences how the wetlands storage influence runoff generation. Here, it is worth noting that even though wetlands cover only a relatively small proportion of the monitored catchment areas (i.e., 13–24%, Table 1), they control the catchments' water production and storage at the ZREO. These findings highlight the importance and the fragility of riparian wetlands as the main – and in this particular case, the only – water storage reservoir in ecosystems where the presence of peaty soil (i.e., Histosols) dominates.

We also identified some $PasS$ variations among our monitored catchments worth highlighting. For instance, even though two of our smaller headwater catchments M1 (0.20 km²) and M2 (0.38 km²) have similar areal proportions covered by wetlands (13–15 %), the smallest catchment M1 showed a much larger $PasS_{(Q)}$ than M2 (394 mm versus 313 mm, respectively). On the other hand, even though catchments M5 (1.40 km²) and M6 (3.28 km²) also have similar wetland coverage (20–22 %), they presented similar $PasS_{(Q)}$ (400–411 mm). These apparent discrepancies likely result from differences in the catchments' average slopes as a metric of topography. For example, the steepest topography of catchment M2 (24%) in relation to M1 (14%) is likely to explain the lowest $PasS_{(Q)}$ of catchment M2. On the contrary, catchments M5 and M6 have similar slopes (18–20%, Table 1), and that factor seems to explain the similar amount of water stored by these catchments. Similar findings have been reported on Scottish peat dominated catchments by Tetzlaff *et al.* (2014). These authors reported that low gradient terrain produced poor drainage conditions, thus, ensuring high volumes of water retained in

Patricio Xavier Lazo Jara

peaty soils throughout the year; whereas steeper terrain that enhances hydraulic gradients allows an enhanced water movement, thus, reducing the amount of water stored in the soils. This combination of factors influencing catchments' *PasS* has also been reported at other studies with different soil types (e.g., Sidle et al., 2001; Lehmann et al., 2007; Detty and McGuire, 2010; Soulsby et al., 2016). Overall, these findings evidence that that even though we did not find a direct relationship between our catchments' average slopes and their $PasS_{(Q)}$ via correlation analysis, catchments' topography exerts controls in the amount of water available for internal mixing.

- *Precipitation controls on dynamic storage*

In the long term, the range of variation of $DynS_{(LT)}$ among catchment was very small (29 – 35mm). As a result, we could not attribute their spatial variability to any of the catchments' features or hydrological variables analyzed in this study. On the other hand, at the event scale, $DynS_{(ES)}$ showed significant correlation with the monitored events' maximum precipitation intensity (Figure 2). This observation suggests that the amount of hydraulically active water linearly increases as the events' maximum intensities increase. This effect likely results from the rapid filling of unsaturated pores in the shallow organic horizon of the páramo soil, which get filled and augment the connectivity of saturated soil patches as precipitation intensity and amount increases (Tromp–van Meerveld and McDonnell, 2006; Tetzlaff *et al.*, 2014). Soulsby *et al.* (2016) found that Histosols at the riparian zones had a rapid filling of stores by precipitation which enhances the connectivity with the hillslopes that increases the *DynS* at the Scottish Girnock catchment that has very similarities with the ZREO. This effect is also seen at our catchment causing a rapid activation of the soils' little *DynS* available, and which in turn results in a rapid delivery of water towards the stream network during rainfall events.

5. Conclusions

Our findings can be summarized in the context of the celerity of the water flux and velocity of a tracer in a hydrologic system. Celerity is related to the propagation speed of a perturbation within a hydrologic system and velocity as the mass flux of a given tracer (McDonnell and Beven, 2014; Beven and Davies, 2015). In these sense, the rapid response of streamflow to precipitation inputs during rainfall events, i.e., the systems celerity, appears to be controlled by the precipitation intensity that rapidly infills the relatively small available páramo soils pore space and causes a rapid discharge response. On the other hand, the attenuation of the stable isotopic composition in streamflow in relation to precipitation (Mosquera *et al.*, 2016a) and the relatively high catchments' *PasS* in the organic horizon of the soils at the ZREO evidence that the velocity of the system is rather dictated by the high water retention capacity of the páramo wetlands (i.e., Histosol soils). As a result, when precipitation intensities increase, the system's celery perturbation is enhanced, and, thus, causes a rapid response in the little available *DynS* (minutes to hours), despite the efficient mixing of tracer in the wetlands, which in turn causes water to be retained in the hydrologic systems from weeks to months. These findings highlighting the vulnerability that changes in land use and climate, both likely to affect the current hydropedological conditions of the páramo soils, could impact the ecosystem's water production and storage capacities and therefore, the importance of managing and preserving this fragile ecosystem

Our evaluation of different methods to estimate *PasS* evidenced that the streamflow mean transit time based method ($PasS_{(Q)}$) provided an accurate estimate in comparison to the hydrophysical soil properties $PasS_{(HP)}$ and soil water MTT based $(PasS_{(S)})$ methods. In addition, for a catchment with an additional contribution from a shallowly sourced spring water, the application of the $PasS_{(Q)}$ and $PasS_{(HP)}$ methods allowed for the estimation of the *PasS* contributed by this additional water reservoir. These results shed new light into the usefulness of both the $PasS_{(Q)}$ and $PasS_{(HP)}$ methods to provide indirect *PasS* groundwater estimations at other catchments with relatively homogeneous soil conditions, where the soils´ hydrophysical properties can be readily characterized.

Patricio Xavier Lazo Jara

6. References

Allen R, Pereira L, Raes D, Smith M. 1998. Crop evapotranspiration-Guidelines for computing crop water requirements-FAO Irrigation and drainage paper 56. *FAO, Rome*

Amvrosiadi N, Seibert J, Grabs T, Bishop K. 2017. Water storage dynamics in a till hillslope: the foundation for modeling flows and turnover times. *Hydrological Processes* **31** (1): 4–14 DOI: 10.1002/hyp.11046

Asbjornsen H, Manson RH, Scullion JJ, Holwerda F, Mu?oz-Villers LE, Alvarado-Barrientos MS, Geissert D, Dawson TE, McDonnell JJ, Bruijnzeel LA. 2017. Interactions between payments for hydrologic services, landowner decisions, and ecohydrological consequences: synergies and disconnection in the cloud forest zone of central Veracruz, Mexico. *Ecology and Society* **22** (2): art25 DOI: 10.5751/ES-09144-220225

Beven K, Davies J. 2015. Velocities, celerities and the basin of attraction in catchment response. *Hydrological Processes* **29** (25): 5214–5226 DOI: 10.1002/hyp.10699

Birkel C, Soulsby C. 2016. Linking tracers, water age and conceptual models to identify dominant runoff processes in a sparsely monitored humid tropical catchment. *Hydrological Processes* **30** (24): 4477–4493 DOI: 10.1002/hyp.10941

Birkel C, Soulsby C, Tetzlaff D. 2011. Modelling catchment-scale water storage dynamics: reconciling dynamic storage with tracer-inferred passive storage. *Hydrological Processes* **25** (25): 3924–3936 DOI: 10.1002/hyp.8201

Bishop K, Seibert J, Nyberg L, Rodhe A. 2011. Water storage in a till catchment. II: Implications of transmissivity feedback for flow paths and turnover times. *Hydrological Processes* **25** (25): 3950–3959 DOI: 10.1002/hyp.8355

Boll J, Selker JS, Nijssen BM, Steenhuis TS, Van Winkle J, Jolles E. 1991. Water quality sampling under preferential flow conditions. In *Lysimeters for Evapotranspiration and Environmental Measurements*, Allen, R.G., Howell, T.A., Pruitt, W.O., Walter, I.A., Jensen ME (ed.).American Society of Civil Engineers: New York; 290–298.

Boll J, Steenhuis TS, Selker JS. 1992. Fiberglass Wicks for Sampling of Water and Solutes in the Vadose Zone. *Soil Science Society of America Journal* **56** (3): 701 DOI: 10.2136/sssaj1992.03615995005600030005x

Botter G, Porporato A, Rodriguez-Iturbe I, Rinaldo A. 2009. Nonlinear storage-discharge relations and catchment streamflow regimes. *Water Resources Research* **45** (10) DOI: 10.1029/2008WR007658

Brauer CC, Teuling AJ, Torfs PJJF, Uijlenhoet R. 2013. Investigating storage-discharge relations in a lowland catchment using hydrograph fitting, recession analysis, and soil moisture data. *Water Resources Research* **49** (7): 4257–4264 DOI: 10.1002/wrcr.20320

Buttle JM. 2016. Dynamic storage: a potential metric of inter-basin differences in storage properties. *Hydrological Processes* **30** (24): 4644–4653 DOI: 10.1002/hyp.10931

Buytaert W. 2004. The properties of the soils of the south Ecuadorian páramo and the impact of land use changes on their hydrology.Katholieke Universiteit Leuven.

Buytaert W, Beven K. 2011. Models as multiple working hypotheses: hydrological simulation of tropical alpine wetlands. *Hydrological Processes* **25** (11): 1784–1799 DOI: 10.1002/hyp.7936

Coltorti M, Ollier C. 2000. Geomorphic and tectonic evolution of the Ecuadorian Andes. *Geomorphology* **32** (1): 1–19 DOI: 10.1016/S0169-555X(99)00036-7

Córdova M, Carrillo-Rojas G, Crespo P, Wilcox B, Célleri R. 2015. Evaluation of the Penman-

Patricio Xavier Lazo Jara

Monteith (FAO 56 PM) Method for Calculating Reference Evapotranspiration Using Limited Data. *http://dx.doi.org/10.1659/MRD-JOURNAL-D-14-0024.1*

Correa A, Windhorst D, Crespo P, Célleri R, Feyen J, Breuer L. 2016. Continuous versus event-based sampling: how many samples are required for deriving general hydrological understanding on Ecuador's páramo region? *Hydrological Processes* **30** (22): 4059–4073 DOI: 10.1002/hyp.10975

Correa A, Windhorst D, Tetzlaff D, Crespo P, Célleri R, Feyen J, Breuer L. 2017. Temporal dynamics in dominant runoff sources and flow paths in the Andean Páramo. *Water Resources Research* **53** (7): 5998–6017 DOI: 10.1002/2016WR020187

Craig H. 1961. Standard for Reporting Concentrations of Deuterium and Oxygen-18 in Natural Waters. *Science (New York, N.Y.)* **133** (3467): 1833–4 DOI: 10.1126/science.133.3467.1833

Crespo P, Bücker A, Feyen J, Vaché KB, Frede H-G, Breuer L. 2012. Preliminary evaluation of the runoff processes in a remote montane cloud forest basin using Mixing Model Analysis and Mean Transit Time. *Hydrological Processes* **26** (25): 3896–3910 DOI: 10.1002/hyp.8382

Crespo PJ, Feyen J, Buytaert W, Bücker A, Breuer L, Frede H-G, Ramírez M. 2011. Identifying controls of the rainfall–runoff response of small catchments in the tropical Andes (Ecuador). *Journal of Hydrology* **407** (1–4): 164–174 DOI: 10.1016/j.jhydrol.2011.07.021

Creutzfeldt B, Troch PA, Güntner A, Ferré TPA, Graeff T, Merz B. 2014. Storage-discharge relationships at different catchment scales based on local high-precision gravimetry. *Hydrological Processes* **28** (3): 1465–1475 DOI: 10.1002/hyp.9689

Davies JAC, Beven K. 2015. Hysteresis and scale in catchment storage, flow and transport. *Hydrological Processes* **29** (16): 3604–3615 DOI: 10.1002/hyp.10511

Detty JM, McGuire KJ. 2010. Threshold changes in storm runoff generation at a till-mantled headwater catchment. *Water Resources Research* **46** (7) DOI: 10.1029/2009WR008102

Dunn SM, Birkel C, Tetzlaff D, Soulsby C. 2010. Transit time distributions of a conceptual model: their characteristics and sensitivities. *Hydrological Processes* **24** (12): 1719–1729 DOI: 10.1002/hyp.7560

FAO. 2009. *Guidelines for soil description.* Food and Agriculture Organization of the United Nations.

Fovet O, Ruiz L, Hrachowitz M, Faucheux M, Gascuel-Odoux C. 2015. Hydrological hysteresis and its value for assessing process consistency in catchment conceptual models. *Hydrology and Earth System Sciences* **19** (1): 105–123 DOI: 10.5194/hess-19-105-2015

Geris J, Tetzlaff D, McDonnell J, Soulsby C. 2015a. The relative role of soil type and tree cover on water storage and transmission in northern headwater catchments. *Hydrological Processes* **29** (7): 1844–1860 DOI: 10.1002/hyp.10289

Geris J, Tetzlaff D, McDonnell JJ, Soulsby C. 2017. Spatial and temporal patterns of soil water storage and vegetation water use in humid northern catchments. *Science of The Total Environment* **595** (April): 486–493 DOI: 10.1016/j.scitotenv.2017.03.275

Geris J, Tetzlaff D, Soulsby C. 2015b. Resistance and resilience to droughts: hydropedological controls on catchment storage and run-off response. *Hydrological Processes* **29** (21): 4579–4593 DOI: 10.1002/hyp.10480

Grant L, Seyfried M, McNamara J. 2004. Spatial variation and temporal stability of soil water in a snow-dominated, mountain catchment. *Hydrological Processes* **18** (18): 3493–3511 DOI: 10.1002/hyp.5798

Hailegeorgis TT, Alfredsen K, Abdella YS, Kolberg S. 2016. Evaluation of storage–discharge relationships and recession analysis-based distributed hourly runoff simulation in large-scale, mountainous and snow-influenced catchment. *Hydrological Sciences Journal* **61** (16): 2872–

Patricio Xavier Lazo Jara

2886 DOI: 10.1080/02626667.2016.1170939

Hale VC, McDonnell JJ, Stewart MK, Solomon DK, Doolitte J, Ice GG, Pack RT. 2016. Effect of bedrock permeability on stream base flow mean transit time scaling relationships: 2. Process study of storage and release. *Water Resources Research* **52** (2): 1375–1397 DOI: 10.1002/2015WR017660

Hasan S, Troch PA, Bogaart PW, Kroner C. 2008. Evaluating catchment-scale hydrological modeling by means of terrestrial gravity observations. *Water Resources Research* **44** (8) DOI: 10.1029/2007WR006321

Heidbüchel I, Güntner A, Blume T. 2015. Use of cosmic ray neutron sensors for soil moisture monitoring in forests. *Hydrology and Earth System Sciences Discussions* **12** (9): 9813–9864 DOI: 10.5194/hessd-12-9813-2015

Hofstede RGM, Mena V, Segarra P. 2003. Los Paramos del Mundo

Holder MW, Brown KW, Thomas JC, Agency USEP, Development USEPAO of R and, Vegas EMSL Las, Nev. 1989. *Development of a Capillary Wick Unsaturated Zone Pore Water Sampler*. Environmental Monitoring Systems Laboratory, Office of Research and Development, United States Environmental Protection Agency.

van Huijgevoort MHJ, Tetzlaff D, Sutanudjaja EH, Soulsby C. 2016. Using high resolution tracer data to constrain water storage, flux and age estimates in a spatially distributed rainfall-runoff model. *Hydrological Processes* **30** (25): 4761–4778 DOI: 10.1002/hyp.10902

IUCN. 2002. High Andean Wetlands. Gland, Switzerland.

Kettridge N, Waddington JM. 2014. Towards quantifying the negative feedback regulation of peatland evaporation to drought. *Hydrological Processes* **28** (11): 3728–3740 DOI: 10.1002/hyp.9898

Kirchner JW. 2009. Catchments as simple dynamical systems : Catchment characterization , rainfall-runoff modeling , and doing hydrology backward. *Water Resources Research* **45**: 1–34 DOI: 10.1029/2008WR006912

Kirchner JW, Feng X, Neal C. 2000. Fractal stream chemistry and its implications for contaminant transport in catchments. *Nature* **403** (6769): 524–527 DOI: 10.1038/35000537

Knutson JH, Lee SB, Zhang WQ, Selker JS. 1993. Fiberglass Wick Preparation for Use in Passive Capillary Wick Soil Pore-Water Samplers. *Soil Science Society of America Journal* **57** (6): 1474 DOI: 10.2136/sssaj1993.03615995005700060013x

Landon M., Delin G., Komor S., Regan C. 1999. Comparison of the stable-isotopic composition of soil water collected from suction lysimeters, wick samplers, and cores in a sandy unsaturated zone. *Journal of Hydrology* **224** (1–2): 45–54 DOI: 10.1016/S0022-1694(99)00120-1

Lehmann P, Hinz C, McGrath G, Tromp-van Meerveld HJ, McDonnell JJ. 2007. Rainfall threshold for hillslope outflow: an emergent property of flow pathway connectivity. *Hydrology and Earth System Sciences* **11** (2): 1047–1063 DOI: 10.5194/hess-11-1047-2007

Maloszewski P, Zuber A. 1996. Lumped parameter models for the interpretation of environmental tracer data. In *Manual on Mathematical Models in Isotope Hydrogeology. TECDOC-910.*

Małoszewski P, Zuber A. 1982. Determining the turnover time of groundwater systems with the aid of environmental tracers. *Journal of Hydrology* **57** (3–4): 207–231 DOI: 10.1016/0022-1694(82)90147-0

McDonnell JJ, Beven K. 2014. Debates-The future of hydrological sciences: A (common) path forward? A call to action aimed at understanding velocities, celerities and residence time distributions of the headwater hydrograph. *Water Resources Research* **50** (6): 5342–5350 DOI: 10.1002/2013WR015141

Patricio Xavier Lazo Jara

McGuire KJ, McDonnell JJ. 2006. A review and evaluation of catchment transit time modeling. *Journal of Hydrology* **330** (3–4): 543–563 DOI: 10.1016/j.jhydrol.2006.04.020

McGuire KJ, McDonnell JJ, Weiler M, Kendall C, McGlynn BL, Welker JM, Seibert J. 2005. The role of topography on catchment-scale water residence time. *Water Resources Research* **41** (5): n/a-n/a DOI: 10.1029/2004WR003657

Mcnamara JP, Tetzlaff D, Bishop K, Soulsby C, Seyfried M, Peters NE, Aulenbach BT, Hooper R. 2011. Storage as a Metric of Catchment Comparison. *Hydrological Processes* **25** (May): 3364–3371 DOI: 10.1002/hyp.8113

Moore RB. 2004. Introduction to salt dilution gauging for streamflow measurement Part 2: Constant-rate injection. *Streamline Watershed Management Blulletin* **8** (1): 11–15

Mosquera GM, Célleri R, Lazo PX, Vaché KB, Perakis SS, Crespo P. 2016a. Combined Use of Isotopic and Hydrometric Data to Conceptualize Ecohydrological Processes in a High-Elevation Tropical Ecosystem. *Hydrological Processes* DOI: 10.1002/hyp.10927

Mosquera GM, Lazo PX, Célleri R, Wilcox BP, Crespo P. 2015. Runoff from tropical alpine grasslands increases with areal extent of wetlands. *CATENA* **125**: 120–128 DOI: 10.1016/j.catena.2014.10.010

Mosquera GM, Segura C, Vaché KB, Windhorst D, Breuer L, Crespo P. 2016b. Insights into the water mean transit time in a high-elevation tropical ecosystem. *Hydrology and Earth System Sciences* **20** (7): 2987–3004 DOI: 10.5194/hess-20-2987-2016

Nippgen F, McGlynn BL, Emanuel RE. 2015. The spatial and temporal evolution of contributing areas. *Water Resources Research* **51** (6): 4550–4573 DOI: 10.1002/2014WR016719

Padrón RS, Wilcox BP, Crespo P, Célleri R. 2015. Rainfall in the Andean Páramo: New Insights from High-Resolution Monitoring in Southern Ecuador. *Journal of Hydrometeorology* **16** (3): 985–996 DOI: 10.1175/JHM-D-14-0135.1

Peters NE, Aulenbach BT. 2011. Water storage at the Panola Mountain Research Watershed, Georgia, USA. *Hydrological Processes* **25** (25): 3878–3889 DOI: 10.1002/hyp.8334

Pfister L, Martínez-Carreras N, Hissler C, Klaus J, Carrer GE, Stewart MK, McDonnell JJ. 2017. Bedrock geology controls on catchment storage, mixing, and release: A comparative analysis of 16 nested catchments. *Hydrological Processes* **31** (10): 1828–1845 DOI: 10.1002/hyp.11134

Picarro. 2010. ChemCorrect TM -Solving the Problem of Chemical Contaminants in H20 Stable Isotope Research, PICARRO INC, California, USA

Polk MH, Young KR, Baraer M, Mark BG, McKenzie JM, Bury J, Carey M. 2017. Exploring hydrologic connections between tropical mountain wetlands and glacier recession in Peru's Cordillera Blanca. *Applied Geography* **78**: 94–103 DOI: 10.1016/j.apgeog.2016.11.004

Poulenard J, Podwojewski P, Herbillon AJ. 2003. Characteristics of non-allophanic Andisols with hydric properties from the Ecuadorian páramos. *Geoderma* **117** (3): 267–281 DOI: 10.1016/S0016-7061(03)00128-9

Quichimbo P, Tenorio G, Borja P, Cárdenas I, Crespo P, Célleri R. 2012. Efectos sobre las propiedades físicas y químicas de los suelos por el cambio de la cobertura vegetal y uso del suelo: Páramo de Quimsacocha al sur del Ecuador. *Suelos Ecuatoriales* **42** (2): 138–153

Roa-García MC, Weiler M. 2010. Integrated response and transit time distributions of watersheds by combining hydrograph separation and long-term transit time modeling. *Hydrology and Earth System Sciences* **14** (8): 1537–1549 DOI: 10.5194/hess-14-1537-2010

Rosenberg EA, Clark EA, Steinemann AC, Lettenmaier DP. 2012. On the contribution of groundwater storage to interannual streamflow anomalies in the Colorado River basin. *Hydrology and Earth*

Patricio Xavier Lazo Jara

System Sciences Discussions **9** (11): 13191–13230 DOI: 10.5194/hessd-9-13191-2012

Sayama T, McDonnell JJ. 2009. A new time-space accounting scheme to predict stream water residence time and hydrograph source components at the watershed scale. *Water Resources Research* **45** (7): W07401 DOI: 10.1029/2008WR007549

Sayama T, McDonnell JJ, Dhakal A, Sullivan K. 2011. How much water can a watershed store? *Hydrological Processes* **25** (25): 3899–3908 DOI: 10.1002/hyp.8288

Schoeneberger PJ, Wysocki DA, Benham EC, Staff SS. 2012. *Field book for describing and sampling soils, Version 3.0* (Natural Resources Conservation Service, ed.). National Soil Survey Center: Lincoln, NE.

Seyfried MS, Grant LE, Marks D, Winstral A, McNamara J. 2009. Simulated soil water storage effects on streamflow generation in a mountainous snowmelt environment, Idaho, USA. *Hydrological Processes* **23** (6): 858–873 DOI: 10.1002/hyp.7211

Sidle RC, Noguchi S, Tsuboyama Y, Laursen K. 2001. A conceptual model of preferential flow systems in forested hillslopes: evidence of self-organization. *Hydrological Processes* **15** (10): 1675–1692 DOI: 10.1002/hyp.233

Smakhtin V. 2001. Low flow hydrology: a review. *Journal of Hydrology* **240** (3–4): 147–186 DOI: 10.1016/S0022-1694(00)00340-1

Soulsby C, Tetzlaff D. 2008. Towards simple approaches for mean residence time estimation in ungauged basins using tracers and soil distributions. *Journal of Hydrology* **363** (1–4): 60–74 DOI: 10.1016/j.jhydrol.2008.10.001

Soulsby C, Birkel C, Geris J, Dick J, Tunaley C, Tetzlaff D. 2015. Stream water age distributions controlled by storage dynamics and nonlinear hydrologic connectivity: Modeling with high-resolution isotope data. *Water Resources Research* **51** (9): 7759–7776 DOI: 10.1002/2015WR017888

Soulsby C, Birkel C, Tetzlaff D. 2016. Modelling storage-driven connectivity between landscapes and riverscapes: towards a simple framework for long-term ecohydrological assessment. *Hydrological Processes* **30** (14): 2482–2497 DOI: 10.1002/hyp.10862

Soulsby C, Neal C, Laudon H, Burns DA, Merot P, Bonell M, Dunn SM, Tetzlaff D. 2008. Catchment data for process conceptualization: simply not enough? *Hydrological Processes* **22** (12): 2057–2061 DOI: 10.1002/hyp.7068

Soulsby C, Piegat K, Seibert J, Tetzlaff D. 2011. Catchment-scale estimates of flow path partitioning and water storage based on transit time and runoff modelling. *Hydrological Processes* **25** (25): 3960–3976 DOI: 10.1002/hyp.8324

Soulsby C, Tetzlaff D, Hrachowitz M. 2009. Tracers and transit times: windows for viewing catchment scale storage? *Hydrological Processes* **23** (24): 3503–3507 DOI: 10.1002/hyp.7501

Spence C. 2007. On the relation between dynamic storage and runoff: A discussion on thresholds, efficiency, and function. *Water Resources Research* **43** (12): n/a-n/a DOI: 10.1029/2006WR005645

Spence C, Guan XJ, Phillips R. 2011. The Hydrological Functions of a Boreal Wetland. *Wetlands* **31** (1): 75–85 DOI: 10.1007/s13157-010-0123-x

Sprenger M, Tetzlaff D, Tunaley C, Dick J, Soulsby C. 2017. Evaporation fractionation in a peatland drainage network affects stream water isotope composition. *Water Resources Research* **53** (1): 851–866 DOI: 10.1002/2016WR019258

Sproles EA, Leibowitz SG, Reager JT, Wigington PJ, Famiglietti JS, Patil SD. 2015. GRACE storage-runoff hystereses reveal the dynamics of regional watersheds. *Hydrology and Earth System*

Patricio Xavier Lazo Jara

Sciences **19** (7): 3253–3272 DOI: 10.5194/hess-19-3253-2015

Staudinger M, Stoelzle M, Seeger S, Seibert J, Weiler M, Stahl K. 2017. Catchment water storage variation with elevation. *Hydrological Processes* **31** (11): 2000–2015 DOI: 10.1002/hyp.11158

Tetzlaff D, Birkel C, Dick J, Geris J, Soulsby C. 2014. Storage dynamics in hydropedological units control hillslope connectivity, runoff generation, and the evolution of catchment transit time distributions. *Water Resources Research* **50** (2): 969–985 DOI: 10.1002/2013WR014147

Tetzlaff D, Buttle J, Carey SK, van Huijgevoort MHJ, Laudon H, McNamara JP, Mitchell CPJ, Spence C, Gabor RS, Soulsby C. 2015a. A preliminary assessment of water partitioning and ecohydrological coupling in northern headwaters using stable isotopes and conceptual runoff models. *Hydrological Processes* **29** (25): 5153–5173 DOI: 10.1002/hyp.10515

Tetzlaff D, Buttle J, Carey SK, McGuire K, Laudon H, Soulsby C. 2015b. Tracer-based assessment of flow paths, storage and runoff generation in northern catchments: a review. *Hydrological Processes* **29** (16): 3475–3490 DOI: 10.1002/hyp.10412

Tromp-van Meerveld HJ, McDonnell JJ. 2006. Threshold relations in subsurface stormflow: 2. The fill and spill hypothesis. *Water Resources Research* **42** (2) DOI: 10.1029/2004WR003800

Tunaley C, Tetzlaff D, Soulsby C. 2017. Scaling effects of riparian peatlands on stable isotopes in runoff and DOC mobilisation. *Journal of Hydrology* **549**: 220–235 DOI: 10.1016/j.jhydrol.2017.03.056

USDA, NRCS. 2004. *Soil Survey Laboratory Methods Manual: Soil Survey Investigations Report No. 42, Version 4.0, November 2004*. United States Department of Agriculture Natural Resources Conservation Service.

Viviroli D, Dürr HH, Messerli B, Meybeck M, Weingartner R. 2007. Mountains of the world, water towers for humanity: Typology, mapping, and global significance. *Water Resources Research* **43** (7) DOI: 10.1029/2006WR005653

Weiler M, McGlynn BL, McGuire KJ, McDonnell JJ. 2003. How does rainfall become runoff? A combined tracer and runoff transfer function approach. *Water Resources Research* **39** (11): n/a-n/a DOI: 10.1029/2003WR002331

Wright C, Kagawa-Viviani A, Gerlein-Safdi C, Mosquera GM, Poca M, Tseng H, Chun KP. 2017. Advancing ecohydrology in the changing tropics: Perspectives from early career scientists. *Ecohydrology*: e1918 DOI: 10.1002/eco.1918

Patricio Xavier Lazo Jara